International Journal of Solids and Structures 50 (2013) 672–679

Contents lists available at SciVerse ScienceDirect

International Journal of Solids and Structures

journal homepage: www.elsevier.com/locate/ijsolstr

An energy-based dynamic loss hysteresis model for giant magnetostrictive materials

Hao Xu, Yongmao Pei *, Daining Fang *, Shigang Ai

State Key Lab for Turbulence and Complex Systems, College of Engineering, Peking University, Beijing 100871, China

ARTICLE INFO

Article history:
Received 11 May 2012
Received in revised form 23 October 2012
Available online 28 November 2012

Keywords:
Giant magnetostrictive materials
Constitutive model
Dynamic loss
Frequency-dependent hysteresis

ABSTRACT

This paper addresses the development of a magneto-elastic coupling dynamic loss hysteresis model for giant magnetostrictive materials (GMMs). Considering the eddy current loss and anomalous loss, a dynamic constitutive model is proposed to predict the dynamic hysteresis behavior of GMMs. The model is validated by comparing the predicted results with experiments. At first, the frequency effect and anisotropy effect on the domain distribution can be obtained. Moreover, the magnetostriction cannot return to the initial value near the coercive field as the magnetization does with the increasing frequency. It can be explained that the domain distribution changes with the increasing energy loss. The model is benefit for the design and control of GMMs actuators.

1. Introduction

Giant magnetostrictive materials (GMMs) have attracted considerable interests, because they have many excellent properties such as high magnetostriction, low magnetocrystalline anisotropy and high energy coupling factor (Clark et al., 1988; Jiles, 2003; Ma et al., 2006; Mei et al., 1998). Therefore, they have been widely used in magnetomechanical transducers, actuators and adaptive vibration control systems in recent years (Dapino et al., 1998; Smith et al., 2000). However, many experiments have shown that the magnetostrictive effect of GMMs exhibits notable nonlinear characteristic and frequency-dependent hysteresis, which bring great challenges to accurately capture the complicated behaviors of GMMs (Bottauscio et al., 2008; Gao et al., 2008; Moffett et al., 1991; Slaughter et al., 2000). Moreover, the intelligent instruments made with GMMs are usually worked in an environment of alternating magnetic field, in which the influence of dynamic loss cannot be neglected. Thus, a constitutive model appropriate to describe the nonlinear dynamic characteristics for GMMs is quite necessary for the applications.

For several decades, many efforts have been made to model the nonlinear magnetostrictive effect of GMMs. Adly et al. (1991) and Natale et al. (2001) simulated the magnetostrictive behavior of GMMs using the Preisach model which could guarantee minor loop closure; Using the Preisach integral method, Tan and Baras (2004) conveniently described the frequency-dependent hysteretic behavior of GMMs; However these models lacked physical meaning and couldnot explain the mechanism of magnetostriction. Jiles and Atherton (1986) proposed a phenomenological model based on the domain wall theory to investigate the hysteresis mechanisms in ferromagnets. Furthermore, Dapino et al. (2000) developed this model to quantify the strains and displacements output by the magnetostrictive transducers. Some other extended models which could describe the dynamic behavior and magnetoelastic coupling effect for GMMs were obtained by considering the eddy current loss (Huang et al., 2007; Wang and Zhou, 2010). It has to be noted that this kind of models assumed that the magnetostriction λ and magnetization M approximately satisfied the relationship $\lambda \propto M^2$. As a result, the value of the magnetostriction was totally controlled by magnetization. Smith et al. (2003) proposed a free energy model which could automatically ensure the closure of biased, nested, minor loops under quasi-static or low exciting frequency; Armstrong (2003) set up an quasi-static anisotropic hysteretic model by introducing an energy based domain distribution mechanism with defect pining energy; Adopting the similar approach, Evans and Dapino (2009) presented an efficient low-order constitutive model for cubic GMMs by directly minimizing the enthalpy to find the most likely domain orientations. However, these models neglected eddy current effect which would cause frequency-dependent hysteresis of GMMs. Then they developed a fully-coupled finite-element dynamic model for 3-D magnetostrictive transducers by coupling Maxwell's equations to Newton's second law (Evans and Dapino, 2011). The model simultaneously quantifies the effects of eddy currents, structural dynamics, and flux leakage on transducer performance.

In this paper, based on the Armstrong quasi-static model, an energy-based magneto-elastic coupling dynamic model of GMMs is established by taking into account the dynamic loss. We reveal the prestress effect and frequency effect on the magnetostrictive effect of GMMs. In addition, the changes of different kinds of energy losses with the increasing exciting frequency are obtained. Moreover, the

* Corresponding authors. Tel.: +86 10 62757417.
E-mail addresses: peiym@pku.edu.cn (Y. Pei), fangdn@pku.edu.cn (D. Fang).

0020-7683/$ - see front matter © 2012 Elsevier Ltd. All rights reserved.
http://dx.doi.org/10.1016/j.ijsolstr.2012.10.029

predicting results indicate that the magnetostriction cannot return to the initial value near the coercive field with the increasing frequency. Then the explanation of this phenomenon is given in terms of domain distribution mechanism.

2. Anhysteretic constitutive theory

Based on the Armstrong incremental model, a three-dimensional anisotropic model is chosen to deeply understand the magnetization mechanism of GMMs. We consider that the GMMs consist of a series of domains, and the internal interaction among the domains is ignored for simplicity as some previous researches. (Jiles and Thoelke, 1994).

In a process of magnetization, the free energy can be written as

$$E_t = E_k + E_\sigma + E_H + E_d \tag{1}$$

where E_k, E_σ, E_H and E_d are the magnetocrystalline anisotropy energy, stress energy, magnetic field energy and demagnetization field energy, respectively. In the present calculation, the demagnetization field effect will be neglected because it is so small in the experiment for the sample with large aspect ratio. The expressions of these energies can be written as follows:

$$E_k = K_1(\alpha_1^2\alpha_2^2 + \alpha_2^2\alpha_3^2 + \alpha_3^2\alpha_1^2) + K_2\alpha_1^2\alpha_2^2\alpha_3^2 \tag{2}$$

where K_1 and K_2 are the magnetocrystalline anisotropy constants. As in the pseudo-cubic material, K_2 is often neglected. $\alpha_i(i = 1,2,3)$ is the direction cosine of the magnetization with respect to the crystal axis.

$$E_H = \mu_0 H M_s(\alpha_1\beta_1 + \alpha_2\beta_2 + \alpha_3\beta_3) \tag{3}$$

where μ_0 is the coefficient of permeability of free space. H denotes the applied magnetic field and M_s is the saturation magnetization. $\beta_i(i = 1,2,3)$ is the direction cosine of magnetic field with respect of the crystal axis.

$$E_\sigma = -\frac{3}{2}\lambda_{100}(\alpha_1^2\sigma_{11} + \alpha_2^2\sigma_{22} + \alpha_3^2\sigma_{33}) - 3\lambda_{111}(\alpha_1\alpha_1\sigma_{12} + \alpha_2\alpha_3\sigma_{23} + \alpha_1\alpha_3\sigma_{13}) \tag{4}$$

where $\sigma_{ij}(i,j = 1,2,3)$ denotes the component of the applied stress. λ_{100} and λ_{111} are the two magnetostrictive parameters which denote the saturation magnetostriction in the [1 0 0] and [1 1 1] direction, respectively. Therefore, we can evaluate the total free energy as the sum of Eqs. (2), (3) and (4), if we have known the intensity and direction of the magnetic field and the stress state.

Generally, the anhysteretic model assumes that the domain state constantly occupies the lowest free energy orientation. However the results are discontinuous, because it assumes that the domains along one direction produce the identical domain process in the perfect material. Indeed, some domains will retain at their initial directions due to the presence of defects, even when a large amount of equivalent domains have a simultaneous switch (Armstrong, 2003; Pei and Fang, 2010). In a pseudo-cubic material like Terfenol-D, the magnetic moments of domains are constrained by the anisotropy to lie along the eight ⟨1 1 1⟩ easy magnetization directions. Armstrong (2003) assumes that the probability of the occupation of magnetization potential follows an inverse exponential distribution function. The orientation distribution function is given as

$$p_i^{an} = C \cdot Exp(-E_i^t/w) \tag{5}$$

where the subscript i represents a particular ⟨1 1 1⟩ type direction. p_i^{an} and E_i^t are respectively the anhysteretic volume fraction and the total free energy in a particular ⟨1 1 1⟩ easy direction; C is a normalization factor which should be evaluated at each applied field and stress condition. w is the energy distribution parameter. A reduction of w will sharpen the magnetization distribution.

As is known, domain rotation in a process of magnetization will in general result in the change in macroscopically magnetization and strain state. Thus the total anhysteretic magnetization M_{an} and magnetostriction λ in any crystallographic directions can be calculated by summing the projection of M and λ contributed by domains along each of easy directions.

$$M_{an} = \sum_{i=1}^{8} p_i^{an} M_s(\alpha_{i1}\gamma_1 + \alpha_{i2}\gamma_2 + \alpha_{i3}\gamma_3) \tag{6}$$

$$\lambda = \sum_{i=1}^{8} p_i^{an}\left\{\frac{3}{2}\lambda_{100}(\alpha_{i1}^2\gamma_1^2 + \alpha_{i2}^2\gamma_2^2 + \alpha_{i3}^2\gamma_3^2) + 3\lambda_{111}(\alpha_{i1}\alpha_{i2}\gamma_1\gamma_2 + \alpha_{i2}\alpha_{i3}\gamma_2\gamma_3 + \alpha_{i3}\alpha_{i1}\gamma_3\gamma_1)\right\} \tag{7}$$

where $\alpha_{ij}(j = 1,2,3)$, $\gamma_i(i = 1,2,3)$ are the direction cosines of the domain magnetization along the ith easy direction and the measuring direction with respect of the crystal axis, respectively.

3. Dynamic hysteresis model

In a hypothetical perfect GMMs crystal, the domain wall translation events responsible for observable changes in magnetostriction and magnetization would occur completely reversibly. However, in the process of magnetization, there actually exist several kinds of energy losses including the quasi-static dissipated energy and the dynamic energy loss caused by alternative magnetic field (Barbisio et al., 2004; Bertotti, 1985;). The energy balance equation of the magnetization process can be expressed as

$$E = E_{sta} + L_{pin} + L_e + L_a \tag{8}$$

here E, E_{sta}, L_{pin}, L_e and L_a stand for the work done per unit volume by the applied magnetic field, the magnetic energy stored in the material, the hysteresis loss per unit volume to pinning sites, the classical eddy current loss per unit volume, and the anomalous loss per unit volume, respectively. And they can be expressed as follows (Iyer and Krishnaprasad, 2005):

$$E = \mu_0 \int M_{an} dH \tag{9}$$

$$E_{sta} = \mu_0 \int M dH \tag{10}$$

$$L_{pin} = \mu_0 \int k dM \tag{11}$$

$$L_e = \mu_0^2 \frac{D^2}{2\rho\eta} \int \left(\frac{dM}{dt}\right)^2 dt \tag{12}$$

$$L_a = \mu_0^{3/2}\left(\frac{GSV_0}{\rho}\right)^{1/2}\left(\frac{dM}{dt}\right)^{3/2} dt \tag{13}$$

where the non-negative constant k is the coefficient of quasi-static energy loss with dimension of ampere per meter, which is proportional to the pinning sites energy. The parameter D is the feature size of the GMMs sample, for example it represents the thickness for a lamination and the diameter for a cylinder. The parameter ρ is the resistivity with dimension of $\Omega \cdot m$. The dimensionless parameter η and the parameter S are respectively the geometry factor and the cross sectional area of the sample. The parameter G is a dimensionless coefficient measuring the damping effect of the eddy current pattern and V_0 represents the internal potential experienced by domain walls with dimension of ampere per meter (Bertotti, 1985). It should be noted that with the increase of frequency, the induced eddy currents become larger and the permeability develops a radial dependence in the material. As a consequence, the magni-

tude of the magnetic field in a conductive cylinder gradually weakened from the surface to the center, which is called the skin effect. However, the formula manipulation can be very complicated if consider this effect in the model. Therefore, this effect is generally not taken into account when calculating eddy current loss in the previous researches, which assumes a homogeneous magnetic field distribution for simplicity when using Eq. (12).

We also can find that if the dynamic loss is ignored, Eq. (8) will be degenerated to the equation $E = E_{sta} + L_{pin}$, which is the basic energy balance expression for the quasi-static Armstrong hysteresis model (Armstrong, 2003). Replacing $(dM/dt)^2dt$ by $(dM/dt)(dM/dH)dH$ for Eq. (12) gives

$$L_e = \mu_0^2 \frac{D^2}{2\rho\eta} \int \left(\frac{dM}{dt}\right)^2 dt = \mu_0^2 \frac{D^2}{2\rho\eta} \int \left(\frac{dM}{dt}\right)\left(\frac{dM}{dH}\right) dH \tag{14}$$

Replacing $(dM/dt)^{3/2}dt$ by $(dM/dt)^{1/2}(dM/dH)dH$ for Eq. (13) gives

$$\begin{aligned} L_a &= \mu_0^{3/2} \left(\frac{GSV_0}{\rho}\right)^{1/2} \int \left(\frac{dM}{dt}\right)^{3/2} dt \\ &= \mu_0^{3/2} \left(\frac{GSV_0}{\rho}\right)^{1/2} \int \left(\frac{dM}{dt}\right)^{1/2} \left(\frac{dM}{dH}\right) dH \end{aligned} \tag{15}$$

Substituting Eqs. (9), (10), (11), (14) and (15) into Eq. (8), the energy equation can be expressed as

$$\begin{aligned} \mu_0 \int M_{an} dH = \mu_0 \int M dH + \mu_0 \int k \frac{dM}{dH} dH + \mu_0^2 \frac{D^2}{2\rho\eta} \int \left(\frac{dM}{dt}\right)\left(\frac{dM}{dH}\right) dH \\ + \mu_0^{3/2} \left(\frac{GSV_0}{\rho}\right)^{1/2} \int \left(\frac{dM}{dt}\right)^{1/2} \left(\frac{dM}{dH}\right) dH \end{aligned} \tag{16}$$

Differentiating Eq. (16) with respect to H, and then dividing by μ_0 gives

$$\begin{aligned} M_{an} = M + k \frac{dM}{dH} + \mu_0 \frac{D^2}{2\rho\eta} \frac{dM}{dt} \frac{dM}{dH} \\ + \mu_0^{1/2} \left(\frac{GSV_0}{\rho}\right)^{1/2} \left(\frac{dM}{dt}\right)^{1/2} \frac{dM}{dH} \end{aligned} \tag{17}$$

We consider that any change in magnetization dM_i is due to the change of the volume fraction of domains dp_i in the specific easy direction, which gives

$$dM_i = M_s dp_i \tag{18}$$

Treating each of the ⟨1 1 1⟩ type directions independently for simplicity, and taking Eq. (18) into consideration, the energy equation (17) can be modified into (19) after some simple mathematical manipulations.

$$\begin{aligned} p_i^{an} = p_i + k \frac{dp_i}{dH} + M_s \mu_0 \frac{D^2}{2\rho\eta} \left(\frac{dp_i}{dH}\right)^2 \frac{dH}{dt} \\ + M_s^{1/2} \left(\frac{\mu_0 GSV_0}{\rho}\right)^{1/2} \left(\frac{dp_i}{dH}\right)^{3/2} \left(\frac{dH}{dt}\right)^{1/2} \end{aligned} \tag{19}$$

here the anhysteretic volume fraction of domains in this direction p_i^{an} can be calculated by Eq. (5). Eq. (19) also indicates that the eddy current loss and the anomalous loss are proportional to dH/dt and $(dH/dt)^{1/2}$, respectively. Specifically, when the applied magnetic field H is a sinusoidal driving magnetic field with fixed frequency f, these two kinds of loss are respectively proportional to f and $f^{0.5}$.

To calculate the differential Eq. (19) of volume fraction p_i, we use Euler method to translate the differential form to difference quotient which gives:

$$\begin{aligned} \left(\frac{\mu_0 GSV_0}{\rho}\right)^{1/2} \frac{M_s^{1/2}}{\Delta H \cdot \Delta t^{1/2}} \left(p_i^{(j+1)} - p_i^{(j)}\right)^{3/2} + \frac{D^2}{2\rho\eta} \frac{\mu_0 M_s}{\Delta H \cdot \Delta t} \left(p_i^{(j+1)} - p_i^{(j)}\right)^2 \\ + \frac{k}{\Delta H} \left(p_i^{(j+1)} - p_i^{(j)}\right) + p_i^{(j)} - p_i^{(j)an} = 0 \end{aligned} \tag{20}$$

where the subscript j is the recurrence step. Therefore if we have known the initial value of applied magnetic field $H^{(0)}$, the initial volume fraction of domains in a specific ⟨1 1 1⟩ direction $p_i^{(0)}$, the magnetic field increment ΔH and the time increment Δt, then the nonlinear equation about $\left(p_i^{(j+1)} - p_i^{(j)}\right)$ can be solved numerically using the Newton–Raphson method.

After the volume fraction p_i is obtained, we can calculate the total magnetization M and magnetostriction λ by substituting the value of p_i to p_i^{an} in Eq. (6) and Eq. (7). Thus we have constructed a non-linear dynamic hysteretic model with dynamic loss effect for GMMs.

4. Experiment verification and discussions

In this paper, in order to verify the validity of the obtained dynamic model, a Terfenol-D rod subjected to compressive prestress

Table 1
Properties of Terfenol-D rod and model parameters.

M_s (A/m)	0.765×10^6	η	16
K_1 (J/m^3)	-0.06×10^6	D (mm)	12.7
λ_{100} (m/m)	90×10^{-6}	k (A/m)	6000
λ_{111} (m/m)	1640×10^{-6}	w (J/m^3)	9000
ρ (Ω/m)	3.5×10^{-6}	V_0 (A/m)	10
G	0.1356		

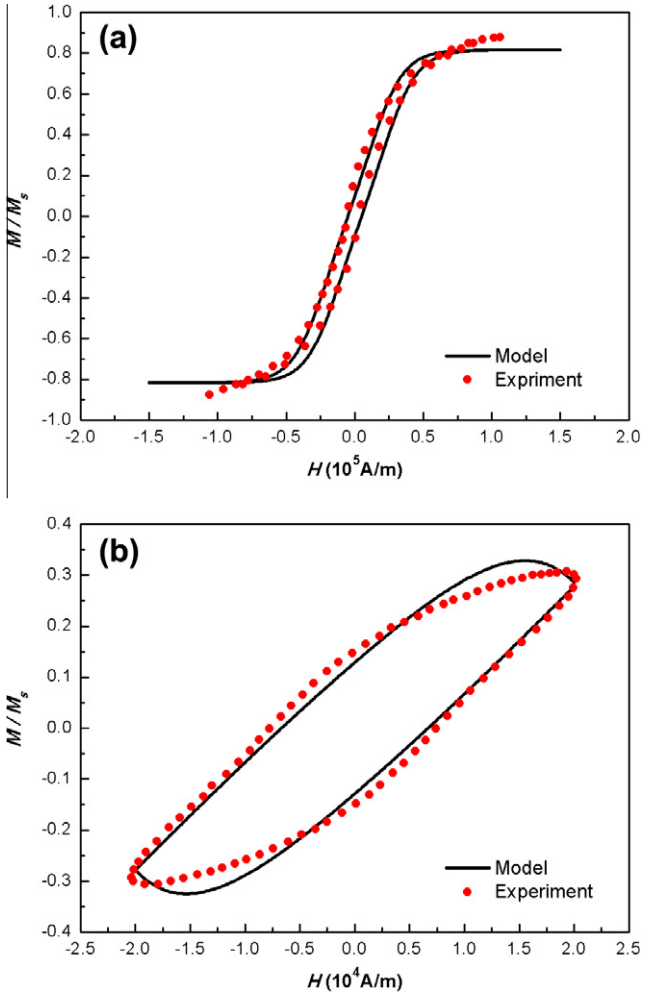

Fig. 1. Comparisons of magnetic hysteresis loops between experimental data and model results under prestress $\sigma = -10.35$ MPa: (a) the exciting frequency $f = 1$ Hz; (b) the exciting frequency $f = 1000$ Hz.

and alternating magnetic field is taken as an example. The parameters used in this model can be summarized as:

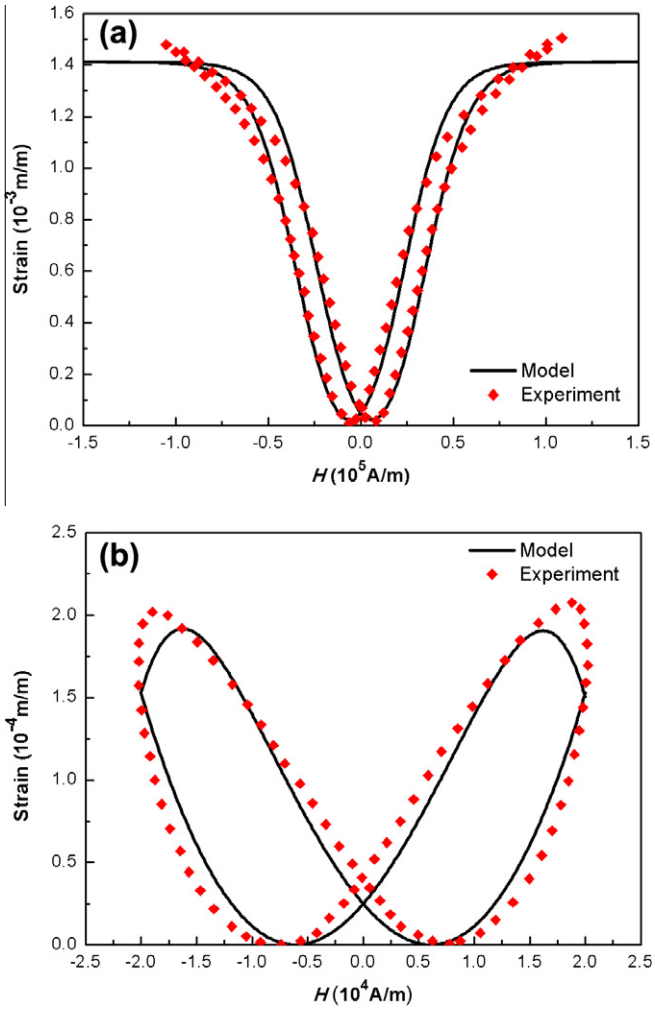

Fig. 2. Comparisons of magnetostrictive curves between experimental data and model results under prestress $\sigma = -10.35$ MPa: (a) the exciting frequency $f = 1$ Hz; (b) the exciting frequency $f = 1000$ Hz.

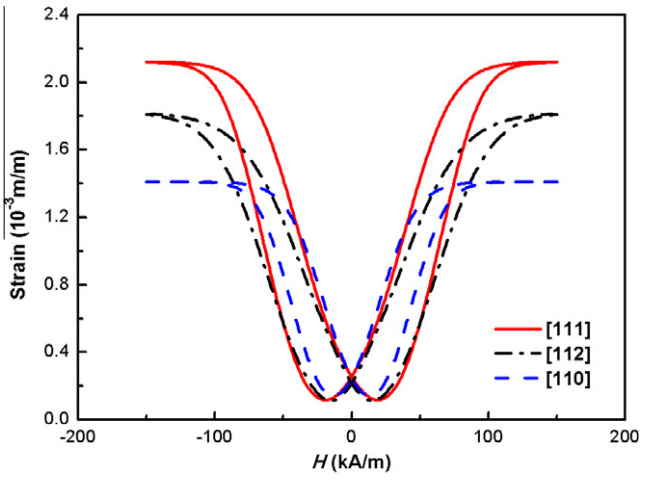

Fig. 3. Simulation of magnetostrictive curves under different directions of applying magnetic field with fixed prestress $\sigma = -10$ MPa for the exciting frequency $f = 1000$ Hz.

(1) Magnetization M_s (measured directly).
(2) Magnetostriction coefficients $\lambda_{100}, \lambda_{111}$ and cubic magnetocystalline anisotropy coefficients K_1 (measured directly, consistent with previously reported values) (Armstrong, 2003).
(3) Coefficient of quasi-static energy loss k (consistent with previous reports, chosen to fit with the experimental data) (Wang and Zhou, 2010).
(4) Energy distribution parameter w (chosen to obtain a good fit with dynamic experimental data).
(5) Parameters to quantify the anomalous loss: G, η and V_0 (consistent with the ferromagnetic loss theory and experiments form Bertotti) (Bertotti, 1985; Wang and Zhou, 2010).

Some properties of the Terfenol-D rod and the adopted physical parameters are given as Table 1. To comply with the experimental conditions (Slaughter et al., 2000), the compressive prestress is taken as 10.35 MPa and the applied magnetic field H is a fixed frequency sinusoidal driving magnetic field [i.e., $H = H_{amp}\sin(2\pi ft)$]. The amplitudes of the applied magnetic field are, respectively, taken as $H_{amp} = 110$ kA/m when the exciting frequency $f = 1$ Hz and $H_{amp} = 20$ kA/m when $f = 1000$ Hz.

The comparisons of magnetic hysteresis loops and magnetostrictive curves under different exciting frequencies between the theoretical results and the experimental data (Slaughter et al., 2000) are, respectively, shown in Figs. 1 and 2. The calculated magnetiza-

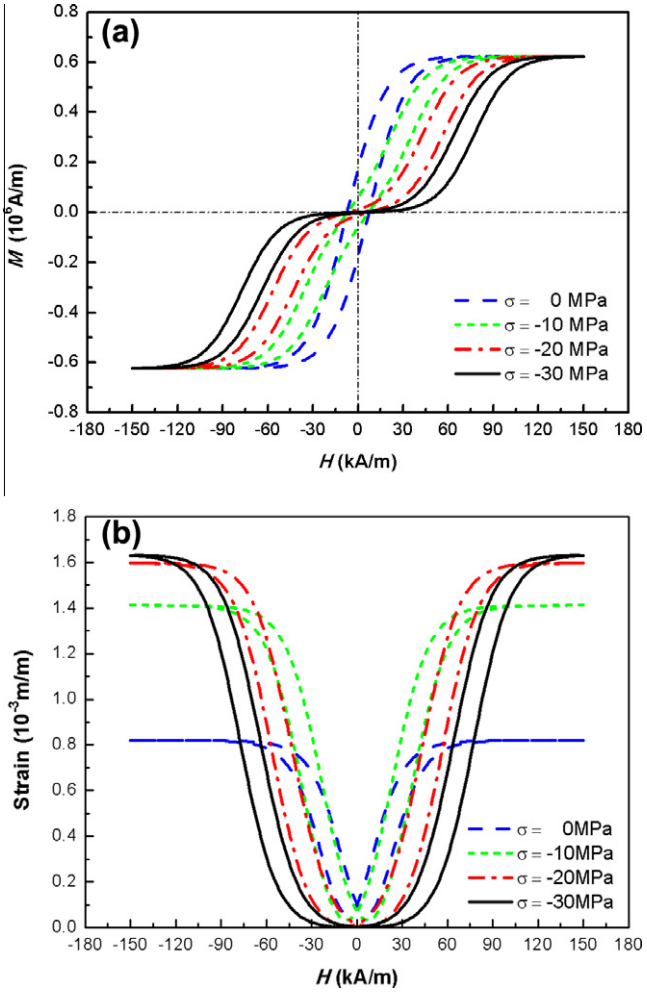

Fig. 4. Simulation of (a) magnetization curves and (b) magnetostrictive curves under different compressive stresses $\sigma = 0, -10, -20, -30$ MPa with fixed exciting frequency $f = 100$ Hz.

tion and magnetostriction, the compressive prestress and the applied magnetic field are all in the [1 1 0] crystallographic direction.

From Figs. 1 and 2, we can see that the present frequency-dependent model results match well with experimental curves, which indicate that the model can effectively describe the dynamic hysteresis characteristics for GMMs. As is evident in these figures, the magnetic hysteresis becomes larger with the frequency increases due to the increasing energy loss. However, there are also some small discrepancies between the measured and reconstructed hysteresis cycles, which can be attributed to the following two facts:

(1) As is known, the total magnetization M is composed of reversible magnetization M_{rev} and irreversible magnetization M_{irr}. The irreversible magnetization results from the energy dissipation during the irreversible domain wall motion, which is the origin of hysteresis. However, the present model is not able to express the changes in relative importance between irreversible and reversible magnetization processes. Thus, some reversible mechanisms occurred in the measurement such as reversible domain wall bowing maybe underestimated in our simulation.

(2) Based on the Armstrong model, we restrict the allowed magnetization to the easy directions, which means domains will only distribute in the ⟨1 1 1⟩ directions that nearest to the [1 1 0] direction in the saturation state. Actually, this ignores the process of domain rotation from ⟨1 1 1⟩ directions to [1 1 0] direction. As a consequence, the calculated saturation magnetization and magnetostriction are smaller than the experimental data in the saturation region. Therefore, the

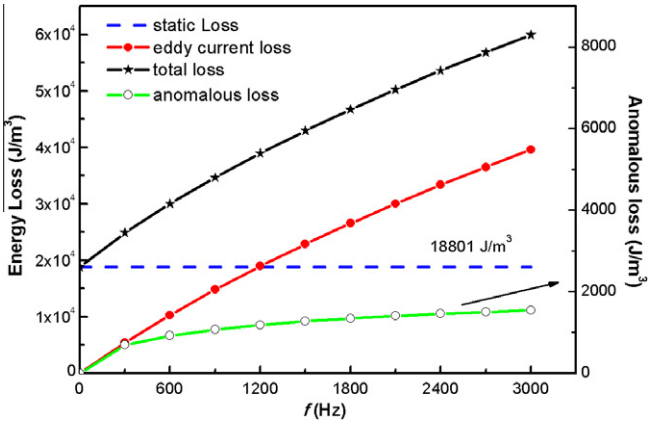

Fig. 6. Different kinds of energy losses per cycle as the function of exciting frequency under compressive stress $\sigma = -10$ MPa.

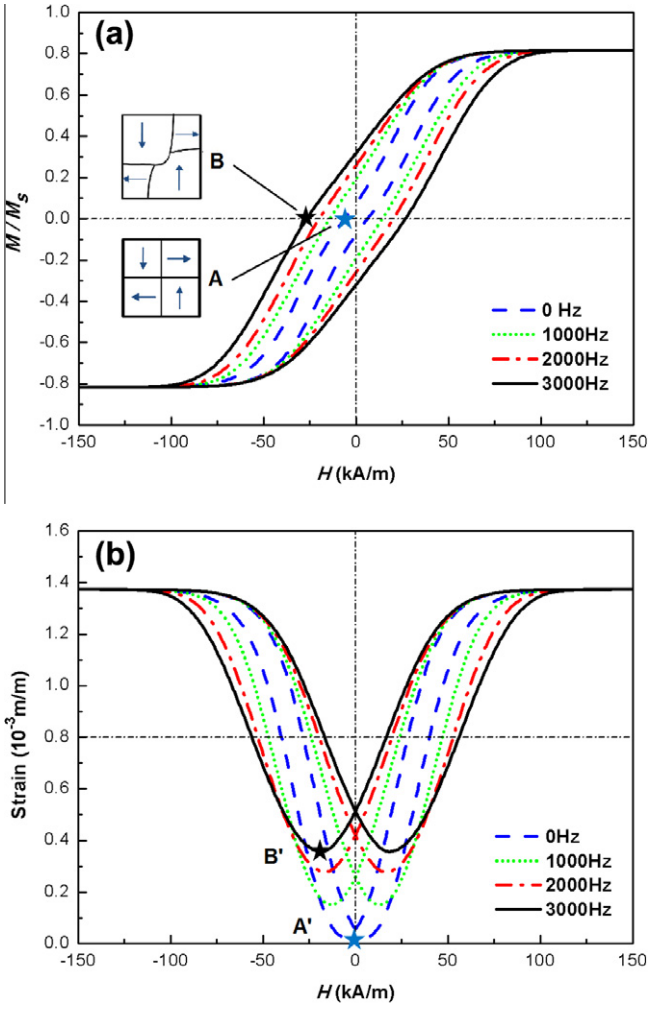

Fig. 5. Simulation of (a) magnetization curves and (b) magnetostrictive curves under different exciting frequencies from 0 to 3000 Hz with fixed prestress $\sigma = -10$ MPa. The simplified schematic of domain distribution near the coercive field is given at Point A (0 Hz) and B (3000 Hz). The Point A′ and B′ in (b) are respectively correspond with Point A and B in (a).

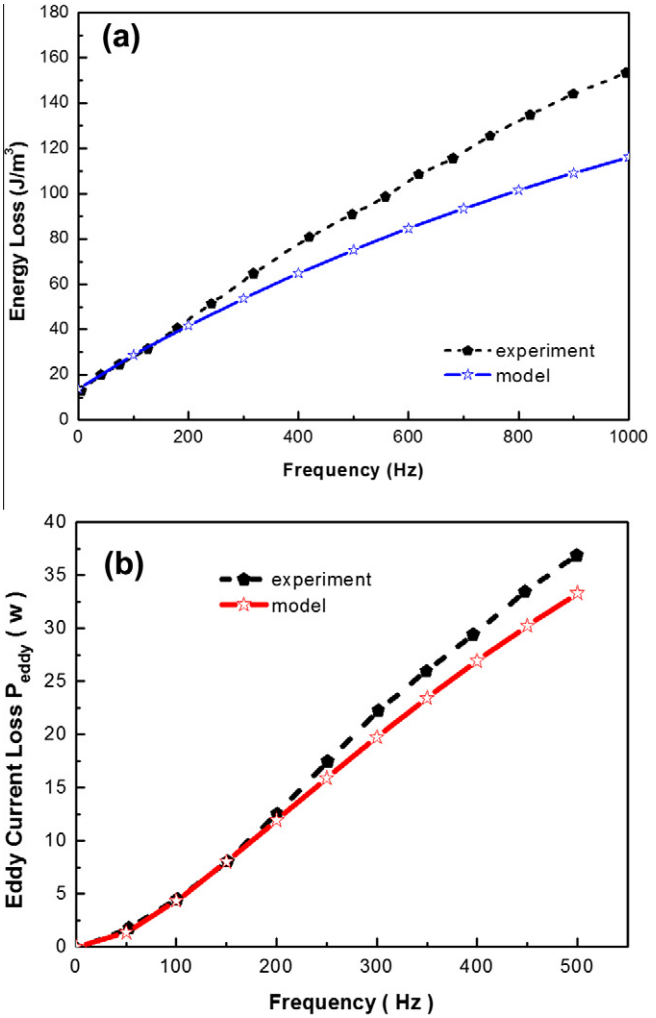

Fig. 7. Measured frequency response of (a) the energy loss per cycle with no prestress at a bias field of 50 kA/m using a 5 kA/m rms drive field and (b) eddy current loss under 20 MPa prestress using a bias field of 40 kA/m and a 24 kA/m drive field (peak to peak) compared with model results.

approach is accurate only when the applied field or stress is aligned with an easy crystal axis, since the easy crystal directions do not rotate. Neglecting domain rotation limits the accuracy of the model, especially when we want to capture the magnetomechanical behavior along a non-easy direction.

The model can also effectively capture the dynamic magnetomechanical behavior of GMMs along different crystallographic directions. As an example, Fig. 3 gives the magnetostrictive curves calculated in different crystal axes. The directions of the applying magnetic field and stress are the same as that of the crystal axis. The simulation shows that the saturated magnetostriction in the [1 1 1] direction is much larger than the other two directions, which is consistent with the experiment conducted by Mei et al. (1998). This can be explained as that the field-induced strain in the [1 1 1] easy direction resulting from the complete rotation of a fully random domain distribution state into the [1 1 1] direction is much larger than that of the [1 1 2] and [1 1 0] directions. In this sense, the Terfenol-D rod oriented to the [1 1 1] crystallographic direction is more suitable for actuators due to its larger saturated magnetostriction under the same compressive prestress.

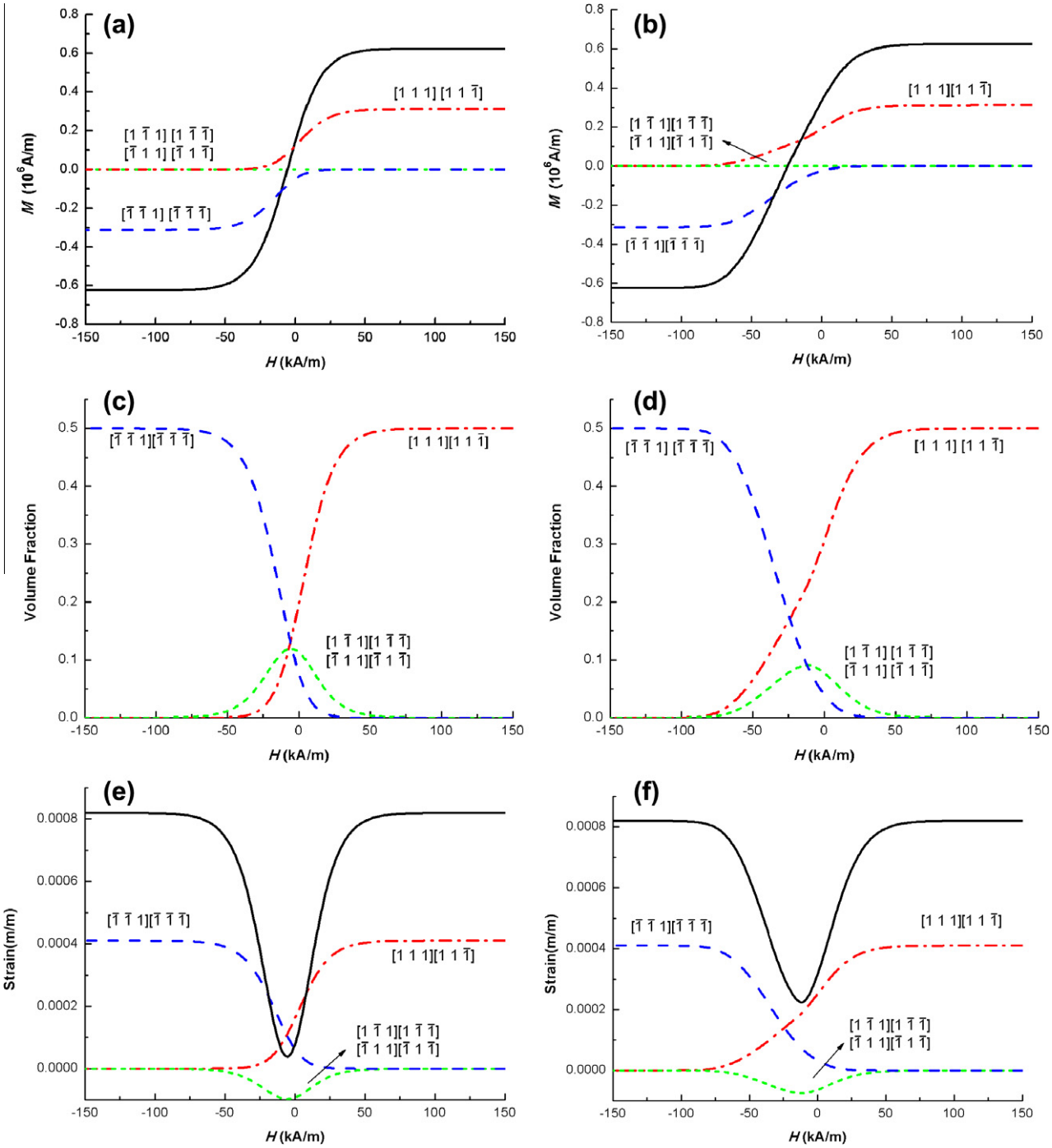

Fig. 8. Simulation of the [(a) and (b)] magnetization, [(c) and (d)] domain volume fractions and [(e) and (f)] magnetostriction with exciting frequency $f = 0$ Hz in [a, c, and e] and $f = 3000$ Hz in [(b), (d), and (f)]. Solid lines are total quantities calculated by summing the contributions by domains from the eight easy directions and dashed/dotted lines correspond to quantities calculated by domains of each single direction.

The magnetization and magnetostriction parallel to the magnetic field direction [1 1 0] under a range of different compressive stresses are predicted in Fig. 4. We study the behaviors of GMMs in this same direction in our latter discussions and analysis. It is evident that the magnetic hysteresis loops exhibit "distortion" under the applied prestress (Clark et al., 1988; Wang et al., 2011). Furthermore, Fig. 4(b) indicates that the applied prestress has remarkable effect on enhancing the saturation magnetostriction. These responses can be attributed to the prestress effect on domain distribution as the previous researches explain (Atulasimha, 2006; Evans, 2009).

The frequency effect on the magnetic hysteresis loops and magnetostrictive curves are shown in Fig. 5. It can be seen that the hysteresis becomes larger as the exciting frequency increases. The reason is that both the eddy current loss and the anomalous loss per cycle increase with the increasing frequency.In order to reflect the frequency effect on the dynamic loss in detail, Fig. 6 gives different kinds of energy losses per cycle as functions of exciting frequency. It is evident that the static loss is frequency independent and the eddy current loss increases with the frequency approximately linearly. When the frequency increases to about 1200 Hz, the eddy current loss reaches almost the same as the static loss about 18801 J/m^3.

Then it gradually plays a leading role in the total energy loss with the increasing frequency. In addition, the anomalous loss increases with the frequency nonlinearly, which is almost less than the other two kinds of losses with one order of magnitude. This suggests that anomalous eddy current behavior, which usually occurs around domain walls, is not significant in this frequency range. This is supported by the fact that domains in Terfenol-D are found to be approximately 10^4 times smaller than the sample diameter, and hence the magnetization in the material behaves nearly homogeneous. However, the anomalous loss cannot be neglected when the static loss is rather small or the exciting frequency is quite high. In conclusion, the eddy current loss and anomalous loss must be incorporated in the model in order to accurately characterize the dynamic hysteresis behavior of GMMs.In addition, comparisons of energy loss per cycle between measurements (Kendall and Piercy, 1993) and model results with no prestress under an applied external magnetic field $H_{ex} = 50 + 5\sqrt{2}\sin(wt)$ (kA/m) are shown in Fig. 7(a). It is evident that a low frequency agreement between the theory and experiment can be obtained. The calculated energy losses given by the analytically model are generally lower than the experimental results. Fig. 7(b) shows the measured frequency response of eddy current loss (Kvarnsjö and Engdahl, 1990) compared with the simulation. To comply with the experimental conditions, the compressive prestress is taken as 20MPa and the applied magnetic field is $H_{ex} = 40 + 24\sin(wt)$ (kA/m).

These calculated results fit the experimentally obtained eddy current losses very well, demonstrating that the energy relations in the model can be well validated.

From Fig. 5 it is also worthwhile to note that, the magnetization can always return to its initial value at the coercive field (Point A and B) with the increase of the frequency, while the magnetostriction cannot (Point A′ and B′). This phenomenon is inconsistent with the results obtained from some dynamic models (Huang et al., 2007; Sun and Zheng, 2006). These models assume that the magnetostriction and magnetization approximately satisfy the relationship $\lambda \propto M^2$, which means the value of magnetostriction is totally controlled by the magnetization. In this case, the magnetostriction can naturally return to its initial value as the magnetization becomes zero at the coercive field. However, as the schematic of domain distribution for Point A and B shows, domains cannot rotate back to their initial distribution states with the increasing frequency. Thus it results in a residual magnetostriction near the coercive field.

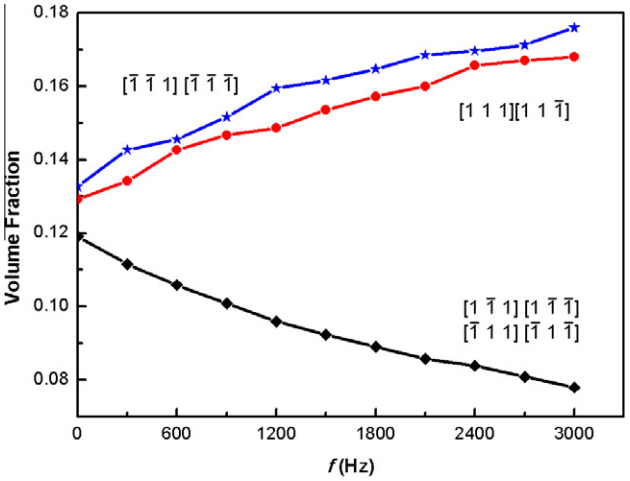

Fig. 9. The volume fractions of domains in different easy directions (near the coercive field) as the function of exciting frequency.

Then we try to explain this interesting phenomenon in terms of domain distribution mechanism. Simulations of the frequency effect on the microcosmic domain distribution of Terfenol-D with no prestress in the [1 1 0] direction are shown in Fig. 8. Fig. 8(a) and (b) indicate that only domain families aligned in the [1 1 1], $[11\bar{1}]$, $[\bar{1}1\bar{1}]$ and $[\bar{1}\bar{1}1]$ directions make contributions to macroscopic magnetization. Moreover, the increase of the frequency decreases the slope of these contributions, which results in an expansionary shift of the total magnetization curve. Therefore, the area of the magnetic loop has a notable increase as well as the coercivity. Fig. 8(d) shows that when the frequency is 3000 Hz, the volume fractions of the domain families in the [1 1 1], $[11\bar{1}]$, $[\bar{1}1\bar{1}]$ and $[\bar{1}\bar{1}\bar{1}]$ directions near the coercive field become larger than that in Fig. 8(c). This can be explained that the increasing energy loss has a significant influence on the domain distribution. Thus, the magnetostriction in Fig. 8(f) cannot return to its initial zero value near the coercive field as Fig. 8(e) exhibits.

Fig. 9 gives the change of domain distribution near the coercive field with the increasing exciting frequency. It can be seen that the volume fractions of domains aligned in the directions perpendicular to the rod axis decrease with the increasing frequency. On the contrary, the volume fractions of domains start from the other four easy directions which contributed to the positive magnetostriction increase gradually. This consequently results in a remarkable residual macroscopic magnetostriction near the coercive field. The interesting phenomenon is consistent with the experiment conducted by Bottauscio et al. (2008).

5. Conclusions

Based on the Armstrong quasi-static theory, a dynamic loss model is established for GMMs by considering the eddy current loss and anomalous loss. The model can accurately predict the dynamic magnetostrictive effect for GMMs subjected to alternating magnetic field and prestress. The predicted results agree well with experiment. The model reveals that the eddy current loss gradually dominates the energy loss with the increasing exciting frequency, while the influence of the anomalous loss is not so remarkable. Furthermore, the increase of the energy loss has a significant influence on the domain distribution, which results in the appearance of residual magnetostriction near the coercive field. In summary,

the model has a clear physical meaning, and is convenient to be used for characterization and design of GMMs devices especially under the complex environment of alternating magnetic field.

Acknowledgments

Supported by the National Natural Science Foundation of China under Grant Nos. 11072003 and 11090331, the National Basic Research Program of China under Grant No. 2010CB8327001, and Foundation of the Author of National Excellent Doctoral Dissertation of China (No. 201029).

References

Adly, A.A., Mayergoyz, I.D., Bergqvist, A., 1991. Preisach modeling of magnetostrictive hysteresis. J. Appl. Phys. 69, 5777–5779.

Armstrong, W.D., 2003. An incremental theory of magneto-elastic hysteresis in pseudo-cubic ferro-magnetostrictive alloys. J. Magn. Magn. Mater. 263, 208–218.

Atulasimha, J. 2006. Characterization and modeling of the magnetomechanical behavior of Iron–Gallium alloys. Ph.D Thesis, Department of Aerospace Engineering, University of Maryland, USA.

Barbisio, E., Fiorillo, F., Ragusa, C., 2004. Predicting loss in magnetic steels under arbitrary induction waveform and with minor hysteresis loops. IEEE Trans. Magn. 40, 1810–1819.

Bertotti, G., 1985. Physical interpretation of eddy current losses in ferromagnetic materials. I. Theoretical considerations. J. Magn. Magn. Mater. 134, 143–160.

Bottauscio, O., Chiampi, M., Lovisolo, A., Roccato, P.E., Zucca, M., 2008. Dynamic modeling and experimental analysis of Terfenol-D rods for magnetostrictive actuators. J. Appl. Phys. 103, 1–3, 07F121.

Clark, A.E., Teter, J.P., McMasters, O.D., 1988. Magnetostriction "jumps" in twinned $Tb_{0.3}Dy_{0.7}Fe_{1.9}$. J. Appl. Phys. 63, 3910–3912.

Dapino, M.J., Calkins, F.T., Flatau, A.B. 1998. On identification and analysis of fundamental issues in Terfenol-D transducer modeling. In: Proceedings of the Society of Photo-optical Instrumentation Engineers San Diego, US, 3329, pp. 278–305.

Dapino, M.J., Smith, R.C., Flatau, A.B., 2000. Structural magnetic strain model for magnetostrictive transducers. IEEE Trans. Magn. 36, 545–556.

Evans, P.G. 2009. Nonlinear magnetomechanical modeling and characterization of Galfenol and system-level modeling of Galfenol-based transducers. Ph.D.Thesis, Department of Mechanical Engineering, The Ohio State University, USA.

Evans, P.G., Dapino, M.J., 2009. Efficient model for field-induced magnetization and magnetostriction of Galfenol. J. Appl. Phys. 105 (113901), 1–6.

Evans, P.G., Dapino, M.J., 2011. Dynamic model for 3-D magnetostrictive transducers. IEEE Trans. Magn. 47, 221–230.

Gao, X., Pei, Y.M., Fang, D.N., 2008. Magnetomechanical behaviors of giant magnetostrictive materials. Acta Mech. Solida Sin. 21, 15–18.

Huang, W.M., Wang, B.W., Cao, S.Y., Sun, Y., Weng, L., Chen, H.Y., 2007. Dynamic strain model with eddy current effects for giant magnetostrictive transducer. IEEE Trans. Magn. 43, 1381–1384.

Iyer, R.V., Krishnaprasad, P.S., 2005. On a low-dimensional model for ferromagnetism. Nonlinear Anal. 61, 1447–1482.

Jiles, D.C., 2003. Recent advances and future directions in magnetic materials. Acta Mater. 51, 5907–5939.

Jiles, D.C., Atherton, D.L., 1986. Theory of ferromagnetic hysteresis. J. Magn. Magn. Mater. 61, 48–60.

Jiles, D.C., Thoelke, J.B., 1994. Theoretical modeling of the effects of anisotropy and stress on the magnetiation and magnetostriction of $Tb_{0.3}Dy_{0.7}Fe_2$. J. Magn. Magn. Mater. 134, 143–160.

Kendall, D., Piercy, A.R., 1993. The frequency dependence of eddy current losses in Terfenol-D. J. Appl. Phys. 73, 6174–6176.

Kvarnsjö, L., Engdahl, G., 1990. Examination of eddy current influence on the behavior of a giant magnetostrictive functional unit. J. Appl. Phys. 67, 5010–5012.

Ma, T.Y., Jiang, C.B., Xiao, F., Yu, L.M., Xu, H.B., Pei, Y.M., Fang, D.N., 2006. Magnetomechanical damping capacity of $Tb_{0.36}Dy_{0.64}(Fe_{1-x}T_x)_2$ (T = Co, Mn) alloys. J. Appl. Phys. 100 (023901), 1–6.

Mei, W., Okane, T., Umeda, T., 1998. Magnetostriction of Tb–Dy–Fe crystals. J. Appl. Phys. 84, 6208–6216.

Moffett, M.B., Clark, A.E., Wun-Fogle, M., Linberg, J., Teter, J.P., McLaughlin, E.A., 1991. Characterization of Terfenol-D for magnetostrictive transducers. J. Acoust. Soc. Am. 89, 1448–1455.

Natale, C., Velardi, F., Visone, C., 2001. Identification and compensation of Preisach hysteresis models for magnetostrictive actuators. Phys. B 306, 161–165.

Pei, Y.M., Fang, D.N., 2010. A magnetoelastic model of nonlinear behaviors of Tb–Dy–Fe alloys based on domain rotation. Int. J. Appl. Electrom. 33, 883–889.

Slaughter, J.C., Dapino, M.J., Smith, R.C., Flatau, A.B. 2000. Modeling of a Terfenol-D ultrasonic transducer. In: Proceedings of the Society of Photo-optical Instrumentation Engineers Newport Beach, US, 3985, pp. 366–377.

Smith, R.C., Bouton, C., Zrostlik, R. 2000. Partial and full inverse compensation for hysteresis in smart material systems. In: Proceedings of the American Control Conference Chicago, US, pp. 2750–2754.

Smith, R.C., Dapino, M.J., Seelecke, S., 2003. Free energy model for hysteresis in magnetostrictive transducers. J. Appl. Phys. 93, 458–466.

Sun, L., Zheng, X.J., 2006. Numerical simulation on coupling behavior of Terfenol-D rods. Int. J. Solids Struct. 43, 1613–1623.

Tan, X.B., Baras, J.S., 2004. Modeling and control of hysteresis in magnetostrictive actuators. Automatica 40, 1469–1480.

Wang, T.Z., Zhou, Y.H., 2010. A nonlinear transient constitutive model with eddy current effects for giant magnetostrictive materials. J. Appl. Phys. 108 (123905), 1–9.

Wang, Z.B., Liu, J.H., Jiang, C.B., Xu, H.B., 2011. The stress dependence of magnetostriction hysteresis in TbDyFe [110] oriented crystal. J. Appl. Phys. 109 (123923), 1–5.